

Filtered Tractography: Validation on a Physical Phantom

James G. Malcolm Martha E. Shenton Yogesh Rathi

Psychiatry Neuroimaging Laboratory, Harvard Medical School, Boston, MA
VA Boston Healthcare System, Brockton Division, Brockton, MA

Abstract. This note summarizes a technique that uses tractography to drive the local fiber model estimation. Existing techniques use independent estimation at each voxel so there is no running knowledge of confidence in the estimated model fit. We formulate fiber tracking as recursive estimation: at each step of tracing the fiber, the current estimate is guided by the previous. To do this we perform tractography within a filter framework and use a discrete mixture of Gaussian tensors to model the signal. Starting from a seed point, each fiber is traced to its termination using an unscented Kalman filter to simultaneously fit the local model to the signal and propagate in the most consistent direction. Despite the presence of noise and uncertainty, this provides a causal estimate of the local structure at each point along the fiber. We applied this technique to a phantom simulating several complex pathway interactions and highlight tracts passing through several prescribed seed positions.

1 Introduction

The advent of diffusion weighted magnetic resonance imaging has provided the opportunity for non-invasive investigation of neural architecture. Using this imaging technique, neuroscientists can investigate how neurons originating from one region connect to other regions, or how well-defined these connections may be. For such studies, the quality of the results relies heavily on the method of reconstructing pathways.

A common approach to tractography is to choose a local fiber model and then fit that model at each voxel independent of other voxels. However, tractography is a causal process: we arrive at each new position along the fiber based upon the diffusion found at the previous position. In this note, we treat model estimation and tractography as such by placing this process within a causal filter [1,2]. As we examine the signal at each new position, the filter recursively updates the underlying local model parameters, provides the variance of that estimate, and indicates the direction in which to propagate tractography. Using causal estimation in this way yields inherent path regularization and accurate fiber resolution through branchings and crossings.

2 Method

2.1 Modeling local fiber orientations

To begin estimating within a finite dimensional filter, we model the diffusion signal using a mixture of tensors. This enables estimation directly from the raw signal without separate preprocessing or regularization. At each image voxel, diffusion is mea-

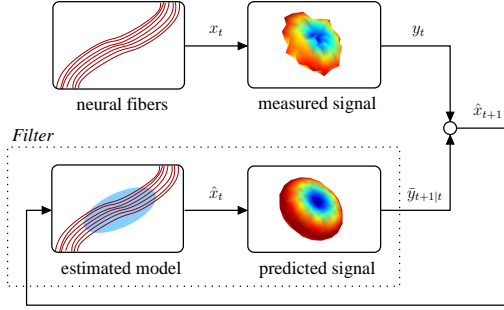


Fig. 1: System overview illustrating relation between the neural fibers, the scanner signal, and the unscented Kalman filter as it is used to estimate the local model. At each step, the filter uses its current estimated model to predict a synthetic signal and then compares that against the actual measured signal from the scanner in order to update its estimated state.

measured along a set of distinct gradients, $\mathbf{u}_1, \dots, \mathbf{u}_m \in \mathbb{S}^2$ (on the unit sphere), producing the corresponding scanner signal, $\mathbf{s} = [s_1, \dots, s_m]^T \in \mathbb{R}^m$. For voxels containing a mixed diffusion pattern, a general weighted formulation is expressed as, $s_i = s_0 \sum_j w_j e^{-b\mathbf{u}_i^T D_j \mathbf{u}_i}$, where s_0 is the baseline signal intensity, b is an acquisition-specific constant, w_j are convex weights, and D_j are tensors, each representing a diffusion pattern.

In this exercise, we begin with the assumption of a mixture of two components. This choice is guided by several previous studies which found two-fiber models to be sufficient at low b -values [3,4,5]. Also, we assume the shape of each tensor to be ellipsoidal, *i.e.* there is one dominant principal diffusion direction \mathbf{m} with eigenvalue λ_1 and the remaining orthonormal directions have equal eigenvalues $\lambda_2 = \lambda_3$ (as in [5,6]). Last, we fix the weights so that each component contributes equally. While assuming equally-weighted compartments may limit flexibility, we found that the eigenvalues adjust to fit the signal in much the same way a fully weighted model would adjust. These assumptions then leave us with the following model used in this work:

$$s_i = \frac{s_0}{2} e^{-b\mathbf{u}_i^T D_1 \mathbf{u}_i} + \frac{s_0}{2} e^{-b\mathbf{u}_i^T D_2 \mathbf{u}_i}, \quad (1)$$

where D_1, D_2 are each expressible as, $D = \lambda_1 \mathbf{m}\mathbf{m}^T + \lambda_2 (\mathbf{p}\mathbf{p}^T + \mathbf{q}\mathbf{q}^T)$, with $\mathbf{m}, \mathbf{p}, \mathbf{q} \in \mathbb{S}^2$ forming an orthonormal basis aligned to the principal diffusion direction \mathbf{m} . The free model parameters are then $\mathbf{m}_1, \lambda_{11}, \lambda_{21}, \mathbf{m}_2, \lambda_{12},$ and λ_{22} . In our current implementation, we restrict each λ to be positive.

2.2 Estimating the fiber model

Given the measured signal at a particular voxel, we want to estimate the underlying model parameters that explain this signal. As in streamline tractography, we treat the fiber as the trajectory of a particle which we trace out. At each step, we propose to trace the local fiber orientations using the estimation at previous positions to guide estimation at the current position. The Kalman filter combines the measured signal with the predicted signal to update the estimated model at the current position. We then move a step in the most consistent direction and repeat this procedure at the new location. Recursive estimation in this manner greatly improves the accuracy of resolving individ-

ual orientations and yields inherently smooth tracts despite the presence of noise and uncertainty. Fig. 1 illustrates this filtering process.

To use a state-space filter for estimating the model parameters, we need the application-specific definition of four filter components:

1. The system state (\mathbf{x}): the model parameters
2. The state transition function (f): how the model changes as we trace the fiber
3. The observation function (h): how the signal appears given a particular model state
4. The measurement (\mathbf{y}): the actual signal obtained from the scanner

For our state, we directly use the parameters for the two-tensor model in Eq. 1:

$$\mathbf{x} = [\mathbf{m}_1 \ \lambda_{11} \ \lambda_{21} \ \mathbf{m}_2 \ \lambda_{12} \ \lambda_{22}]^T, \quad \mathbf{m} \in \mathbb{S}^2, \lambda \in \mathbb{R}^+. \quad (2)$$

For the state transition we assume identity dynamics; the local fiber configuration does not undergo drastic change as it moves from one location to the next. Our observation is the signal reconstruction, $\mathbf{y} = h[\mathbf{x}] = \mathbf{s} = [s_1, \dots, s_m]^T$ using s_i described by the model in Eq. 1, and our measurement is the actual signal interpolated directly on the diffusion weighted images at the current position.

Since our signal reconstruction in Eq. 1 is nonlinear, we employ an unscented Kalman filter to perform estimation. Similar to classical linear Kalman filtering, the unscented version seeks to reconcile the predicted state of the system with the measured state and addresses the fact that these two processes—prediction and measurement—may be nonlinear or unknown. See [7,1,2] for details on this filtering formulation.

3 Results and Discussion

Among the provided phantoms, we present results using the 3mm version at $b = 1500$ [8]. Instead of initializing tractography from the prescribed seed points, we begin by seeding in voxels with nonzero baseline intensity and terminating tractography when the estimate becomes isotropic, essentially “full-brain” tractography. From these potential pathways, Fig. 2 shows a representative fiber for each seed point. We further restricted movement to the image plane.

With the explosion of techniques for mapping connectivity, it is often difficult to assess the relative merits among various approaches, and each application has its particular goals. For connectivity studies, one may only be interested in the final resolved pathway; however, questions arise such as whether to branch or whether to represent connectivity as a discrete path or a voxel-to-voxel connectivity matrix possibly telling more about the relative certainty of connectivity. For tissue studies, one may be primarily concerned with the estimated microstructure at each position. Filtered approaches like this provide not only an estimate of these quantities (mean) but also an additional measure of uncertainty (variance).

The approach presented here may be considered a local method: at the current position we estimate a direction and take a step. With such approaches, one mistake can send the subsequent trajectory off track. We believe that more global approaches should be considered, ones that take into account larger portions of the fiber pathway. Further, we believe that anatomical priors should be incorporated. Such a progression of techniques may be considered analogous to how level set methods developed from local edge-based computations, to more global region-based approaches, and further with integration of shape priors.

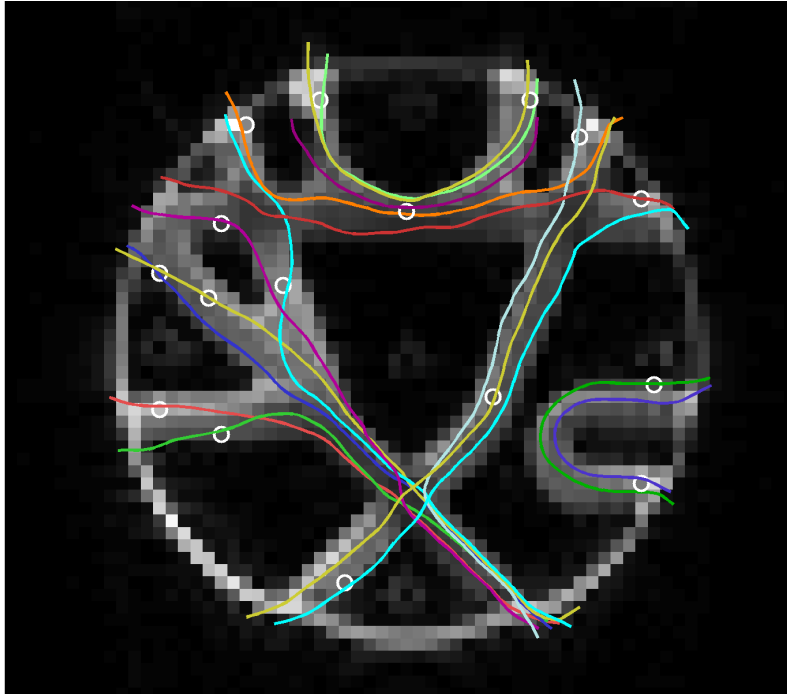


Fig. 2: Baseline image from the synthetic phantom (3mm, $b = 1500$) overlaid with selected fiber tracts (colored) and seed points (white). The filter is capable of tracing through regions of crossing, branching, and fanning.

References

1. Malcolm, J.G., Shenton, M.E., Rathi, Y.: Neural tractography using an unscented Kalman filter. In: Information Processing in Medical Imaging (IPMI). (2009) 126–138
2. Malcolm, J.G., Shenton, M.E., Rathi, Y.: Two-tensor tractography using a constrained filter. In: Medical Image Computing and Computer Assisted Intervention (MICCAI). (2009) 894–902
3. Tuch, D., Reese, T., Wiegell, M., Makris, N., Belliveau, J., Wedeen, V.: High angular resolution diffusion imaging reveals intravoxel white matter fiber heterogeneity. *Magnetic Resonance in Medicine* **48** (2002) 577–582
4. Kreher, B., Schneider, J., Mader, I., Martin, E., Hennig, J., Il'yasov, K.: Multitensor approach for analysis and tracking of complex fiber configurations. *Magnetic Resonance in Medicine* **54** (2005) 1216–1225
5. Peled, S., Friman, O., Jolesz, F., Westin, C.F.: Geometrically constrained two-tensor model for crossing tracts in DWI. *Magnetic Resonance in Medicine* **24**(9) (2006) 1263–1270
6. Kaden, E., Knösche, T., Anwender, A.: Parametric spherical deconvolution: Inferring anatomical connectivity using diffusion MR imaging. *NeuroImage* **37** (2007) 474–488
7. Julier, S., Uhlmann, J.: Unscented filtering and nonlinear estimation. *IEEE* **92**(3) (2004) 401–422
8. Poupon, C., Rieul, B., Kezele, I., Perrin, M., Poupon, F., Mangin, J.F.: New diffusion phantoms dedicated to the study and validation of high-angular-resolution diffusion imaging (HARDI) models. *Magnetic Resonance in Medicine* **60**(6) (2008) 1276–83